Central Pattern Generator for Pneumatic Soft Robots

Johannes Roelf Vegter[a] and Martin Philip Venter[a]

Received 1 June 2023, in revised form 22 August 2024 and accepted 2 May 2025

Abstract: Soft robots open many possibilities to embed intelligence within the structure of a robot. However, central control of external valves and many control lines typifies pneumatic soft robots. This study proposes a soft pneumatic pattern generator to control the activation of two pneumatic actuators simultaneously. The concept mimics biological locomotive control, where nerve clusters distributed throughout the body control the activation of muscle fibres rather than a central brain. The brain sends out relatively simple proportional signals, converted to more intricate patterns locally. Adapting this concept to soft robotics simplifies their typical control requirements. The proposed pattern generator controls two actuators connected to a single pressure supply, resulting in each actuator articulating out of phase with the other. The pressure curves are similar for each output, producing a balanced oscillation of the two actuators. Increasing the supply pressure increases the frequency of oscillation. This configuration is better suited to control symmetric, biomimetic locomotors than previous realisable pneumatic central pattern generators.

Additional keywords: Pattern Generator, Soft Robot, Compliant Materials

1 Introduction

Whether monitoring coral on the Great Barrier Reef [1], picking peaches in the Americas [2] or empowering a person with disabilities to care for themselves for a few more years [3], the field of soft robotics is bridging the gap between the mechanical and biological worlds. Inspired by soft biological organisms such as the octopus [4], worms [5], and caterpillars [6], soft robots are fundamentally different from their more traditional, hard-linked namesakes [7] and cannot necessarily build upon the knowledge gathered from traditional robot design [8].

Although many of the shapes and behaviours observed in soft robotics are biologically inspired, the inspiration does not yet extend to the control of soft robots. Counter to the defining characteristic of soft pneumatic robots, electronic control of hard valves is the most common control method for soft robots [9]. There are, as of yet, few soft control components. In part, the extensive use of non-linear viscoelastic materials results in a lack of predictable behaviour [10, 11, 12], and few sensors can withstand the degree of deformation typical in soft robots [13, 14, 15, 16].

Soft robotics has much to learn from nature, where the locomotive control system uses decentralised neural control mechanisms. The study of neural mechanisms for locomotive control in vertebrates introduces the concept of central pattern generators [17]. The field today uses two common model organisms, the lamprey and the salamander [18, 19, 20, 21]. Each has a simple nervous system that controls its locomotion, with properties of interest to the soft robotics community. Decentralised nerve clusters, known as Central Pattern Generators (CPG), step up simple neural signals to more complex local signals, reduce neural load and signal complexity in small vertebrates such as the salamander.

In biological systems, electric stimulation of the mesencephalic locomotor region of the brain induces the locomotion mode of the salamander to change [22, 23]. Low levels of stimulation induce a trotting gait that increases in speed as the stimulation strength increases. Once the level of stimulation passes a threshold, it induces a swimming gait. In both locomotion modes, the frequency of movement is proportional to stimulation strength. The CPG network runs along the entire length of the spinal cord and is responsible for activating the muscles along the spine. Separate CPGs work in conjunction with each other to enable locomotion.

In 2007, Ijspeert and collaborators successfully replicated this process in a conventional hard-linked robot salamander [24]. A central high-level controller sends a proportional signal to a sequence of CPGs controlling each pair of legs. The CPG provides an oscillating signal to each leg that is 90° out of phase.

Faudzi and colleagues refer to the same salamander gait changes while moving from walking to trotting to swimming gait in their design of a soft amphibious robot [25]. This soft robot successfully mimics the three locomotive gaits of the salamander but does not use central pattern generators and requires the active control of 16 independent actuators.

With soft robots, deformation in response to the loading of the robot or actuator determines behaviour. Tuning the morphology of a soft robot embeds the behaviour as an inherent characteristic of a robot, a form of material intelligence [9, 26]. Which, in some cases, acts as a partial substitute for a central control system, reducing the control requirements of soft robots [27] to yield robots better suited to unstructured environments [28]. The compliant material and design substitute some of the traditional control loops [29], passively achieving the desired behaviour [30].

Where active control cannot be substituted, many contemporary pneumatically actuated soft robots use only binary pressure control [31, 32, 33] involving only the opening and

[a] ORCID 000-0002-0238-0305. Department of Mechanical and Mechatronic Engineering, Stellenbosch University, Joubert Street, Stellenbosch 7602, South Africa, E-mail: mpventer@sun.ac.za

http://dx.doi.org/10.69694/2309-8988/2025/v41a3

closing of electronic or pressure-actuated valves [9, 11, 34]. Often, the switchgear uses hard components placed externally. Some alternative methods used to control soft robots include magnets [35], microfluidics [36, 37, 38, 39, 40, 41], band-pass valve [42], and soft check valves [43], each with its benefits and drawbacks. Microfluidic controllers allow for complex logic but require geometric balancing for each application and provide a limited flow rate [44]. The band-pass valve allows for the control of multiple actuators, but only in a predefined sequence and with limited adaptability. Soft check valves are simple and function well, but are limited to a single switching pressure.

In 2018, Rothemund and coworkers addressed many of the limits imposed by currently available soft-valve designs by proposing a valve based on snap-through of a central diaphragm to hold the valve in one of two states and the choking effect of a buckled tube to seal off the supply [45]. The valve acts as a 2-position, 2-way valve with external pilot control. When supplied with sufficient pressure, the valve switches state. A second pilot line biases the switching pressure, allowing it to be adjusted. This valve allows for binary switching, and the bistability allows for latching of the valve.

A network of Rothmund valves can replicate many of the features needed in a CPG producing N oscillating outputs from a single pressure source using N valves [46]. The oscillation frequency is adjustable and depends on three tunable system parameters. Producing an oscillating signal requires an odd number of complete valves. Using this style of Preston valve network, it is possible to produce a rhythmic control signal suitable for locomotion [47]. With further extension, the work presented by Preston can be extended to a general digital logic for soft devices [48].

To extend on the generalizability presented by Preston, Xu and company present an elegantly simple normally-closed valve with an external pilot that functions as a digital NOT gate [49]. Combinations of the normally closed valve provide the opportunity to create generalised soft pneumatic circuits with scalable complexity. However, without the same level of physical scalability as electronic transistors, the large number of valves needed to implement practical control will limit their utility.

This paper uses buckling tubes, a bi-stable diaphragm, and internal pressure feedback to create an entirely soft, pneumatic oscillator that uses a single constant pressure to generate two out-of-phase output pressures autonomously. The frequency of the oscillating pressure output depends on the input pressure, the volume of air required to activate an attached actuator and the critical load of the buckling tubes. We then demonstrate the use of the soft CPG on a simple two-actuator test case.

This study aims to demonstrate that an adaptation of the Rothemund bi-stable valve can autonomously control airflow through a soft robot in a predictable, tunable way. The CPG structure and switching capability are well-suited to design and fabrication using the same tools and techniques used in cast silicone robots. A reduced switching bias results from an improved snap-through diaphragm. The practical example of the alternating inflation of two soft actuators highlights the utility of the new design.

2 Representation of Related Work

The work presented by Rothemund, Preston, and Xu et al. each contribute to the development of compliant mechanical controllers for pneumatic soft robots. However, they use an unconventional schematic representation for their pneumatic circuits in presenting their work, making it difficult to compare with other similar circuits. Framing their work in a more conventional symbolic system allows better Comparison with each other and existing control circuits.

The convention used in pneumatics shows a horizontal sequence of blocks containing the mapping of external ports in each valve position. To the left and right of the mapping, the method of actuation used to switch between positions. For example, figure 1 shows the "not-gate" symbol used by Xu et al. in contrast to the conventional representation of a pneumatic 2-position, 2-way, normally closed check valve with pilot control and spring return. The figure highlights the convention by indicating the two positions of the valve in the centre and the two activation methods. On the symbol's right, a pilot pressure switches the valve from position 1 to position 2. When the pilot pressure is reduced, the valve returns to position 1 under the action of a spring.

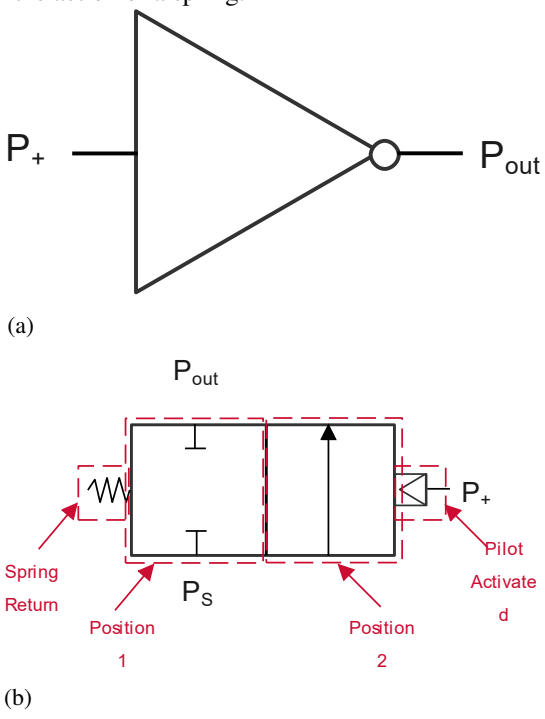

Figure 1 A comparison of the logic symbol used by Xu et al. and an equivalent standard pneumatic symbol. a) Xu's original digital 'NOT-gate' symbol. When the activation signal P_+ is low, the output pressure P_{out} is high and vice versa. b) Xu's circuit using standard pneumatic symbols. Supply pressure P_S, switching pressure P_+, and output pressure P_{out} are indicated. Additional highlights have been added to the pneumatic diagram to explain the layout of the standard symbol—specifically, the two valve positions and the switching mechanisms.

Already evident in the Comparison is the loss of informa-

http://dx.doi.org/10.69694/2309-8988/2025/v41a3

tion in the logic symbol, as it does not directly indicate that the activation and output pressures are not directly connected, and that a functional circuit needs an independent supply pressure.

Rothemund et al. use a similar unconventional schematic representation for their pneumatic circuit. Figure 2 shows the symbol created by Rothemund's group next to an equivalent pneumatic valve symbol. Using the conventional symbols, it is clear that the valve proposed by Rothmunde is a 2-position, 3-way valve with two external pilot lines that can be biased to switch the two positions. In position 1, the supply pressure connects to the valve output, and in position 2, the output can vent to the atmosphere.

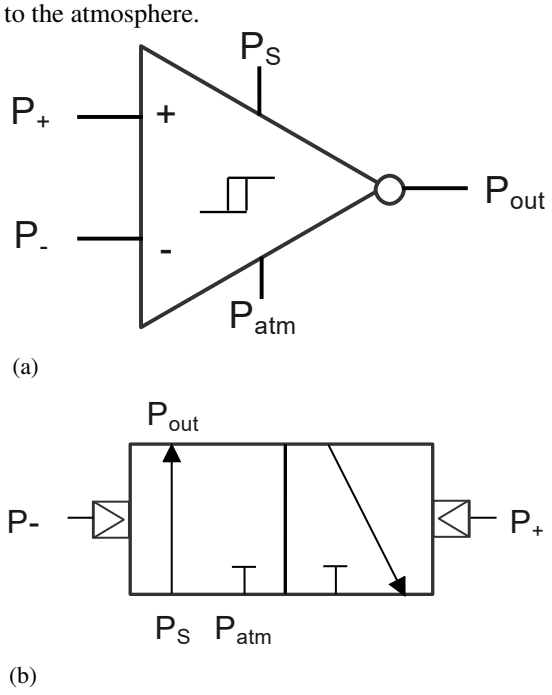

Figure 2 A comparison of a) the symbols used by Rothemund and b) the conventional pneumatic equivalent. Supply pressure P_S, atmospheric pressure P_{atm}, biasing pressures P_+ and P_-, and output pressure P_{out} are each indicated.

The Rothemund symbol contains more information than the Xu symbol in that it acknowledges both the need for supply pressure and the ability to vent to the atmosphere. However, it is clear when comparing the two pneumatic symbols that even though the mechanical design and operation of the Xu and Rothemund devices differ significantly, they are quite similar control components.

Representing the Rothemund oscillator as a pneumatic circuit, Figure 3, shows the same 2-position valve with two external pilots and one spring return (resulting from the bi-stable diaphragm). The valve connects a constant pressure supply to an accumulator (or actuator) in position one. Figure 4 provides clarifying diagrams for the equivalent pneumatic components. Over time, the accumulator pressure increases to a point where the pressure is sufficient to switch a variable pressure relief valve, internally charging the external pilot for the 2-position valve to the second position, allowing the accumulator to vent to the atmosphere. As the pressure in the accumulator decreases, so does the pressure to the pressure relief valve. When the pilot pressure is low enough, the relief valve closes, and the valve returns to position one due to the spring action of the bistable diaphragm. The second pilot is allowed to vent to the atmosphere. This cycle repeats, resulting in the observed oscillating behaviour.

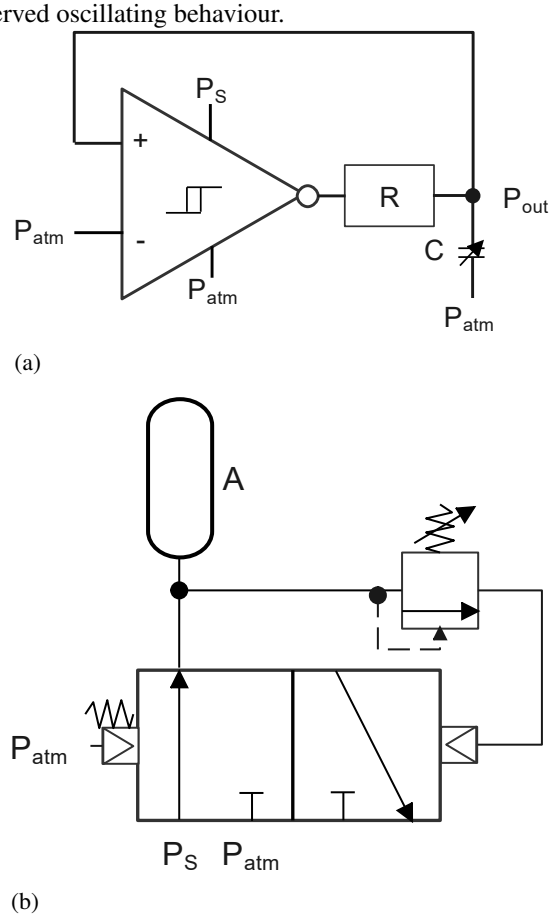

Figure 3 A comparison of a) the symbolic Rothemund oscillator with b) the equivalent pneumatic circuit. Connections to supply pressure P_S and atmospheric pressure P_{atm} are indicated.

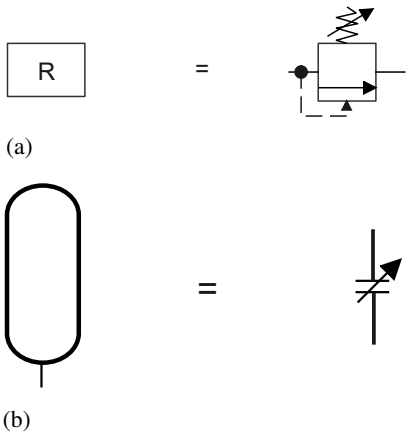

Figure 4 a) and b) show the symbolic equivalents of two additional components labelled "resistance" and "variable capacitor" by Rothemund. As indicated, these are physically represented by a pressure relief valve and an accumulator.

http://dx.doi.org/10.69694/2309-8988/2025/v41a3

Preston et al. propose connecting an odd number of Ruthemund valves in an inverter arrangement. Here, the output of the first valve is the pilot for the second, and so on. When connected to a supply, this leads to a switching cascade. Figure **??** shows the pneumatic circuit for the Preston oscillator next to its Rothemund symbol equivalent.

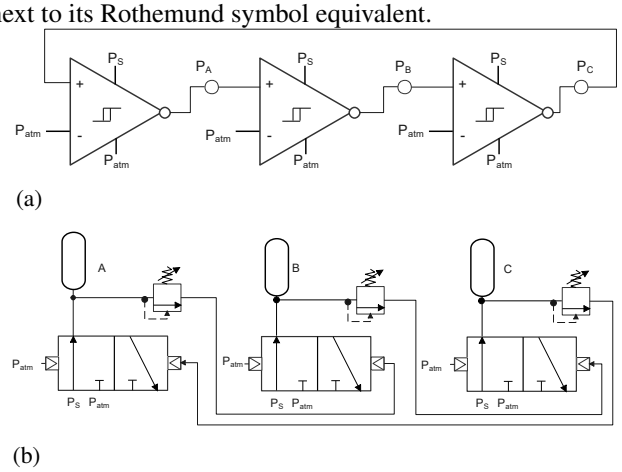

Figure 5 A comparison of a) the symbolic Preston oscillator with b) the equivalent pneumatic circuit. Connections to supply pressure P_S and atmospheric pressure P_{atm} are indicated.

This paper presents a new configuration using a 2-position, 4-way valve rather than the 2-position, 3-way valve used by Rothemund and Preston, and as such cannot be represented using the Rothemund symbols. Unlike either Rothemund or Preston, the proposed circuit controls two actuators with a single valve. The implemented design further does away with the required external pilot to bias the circuit, Figure 6.

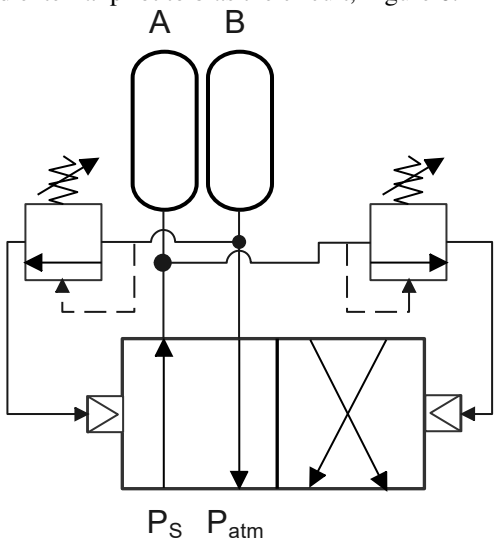

Figure 6 The proposed pneumatic CPG circuit connected to two accumulators (or actuators). Each accumulator connects to a variable pressure relief valve, which activates one of two pilots to switch the valve between two positions. Connections to supply pressure P_S and atmospheric pressure P_{atm} are indicated.

3 Materials and Methods

Two elastomers were considered, Smooth-Sil 950 and Mold Star 30, with a Shore hardness of 50A and 30A, respectively. The fabrication of all parts makes use of casting and 3D printed moulds. During assembly, Sil-Poxy is used to bond the precast parts together. The files for 3D printing of the moulds and the complete fabrication process are available as supplemental materials.

To meet the study objectives requires two experimental setups: 1) determine the critical buckling length for elastomer tubes and 2) test for oscillation. We used a simple carriage and clamp device to determine the critical buckling length of various elastomer tubes. The buckling carriage can test tubes from 20 mm to 45 mm in a fixed-fixed end configuration, figure 7. After clamping a tube into the fixture with the desired initial length (L_0), one end of the tube connects to a pressure-regulated air supply (P_S). Applying a force (F_B) to the carriage slides it along a rail to compress and buckle the tube. When the tube buckles, it pinches closed and stops the flow through the tube. A mechanical vernier calliper with 0.02 mm accuracy measures the compressed length of the tube (L_C).

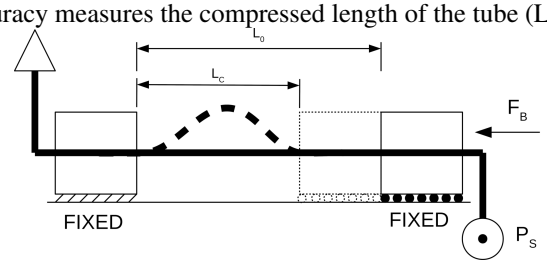

Figure 7 A schematic representation of the carriage and clamp device that was used to determine various elastomer tubes' critical buckling length. The pressure line is connected to one stationary fixed clamp and one sliding clamp with an initial clamped length of L_0. Next, a source pressure P_S is applied, and the sliding clamp is subjected to a buckling load F_B. The critical length L_C is determined at the point where air no longer flows freely through the tube.

The soft CPG is itself tested on a pneumatic bench setup. The CPG functions as a 2-position, 4-way, 4-port pneumatic valve with internal pilot control switching each way. The valve input is connected to a pressure-regulated air supply, while the two outputs connect to an elastomer accumulator. These elastomer accumulators are representative of a soft robotic use case where air flows into an actuator, whose degree of articulation depends on the pressure within. The pressure is measured directly at the input (P_S) and the two output ports (P_A and P_B). All pressure values are measured using a Deltabar M PMD55 (-5 to 50 kPa) pressure transducer and recorded using an HBM QuantumX MX410B Universal Amplifier.

The data are detrended if required, and a single-term Fourier fit was applied to the pressure over time data to estimate the amplitude, frequency and phase for each of the output pressure oscillations. All time-series data were processed using a subset rolling window.

The soft CPGs are composed of buckling tubes that func-

http://dx.doi.org/10.69694/2309-8988/2025/v41a3

tion as pinch valves, a bi-stable diaphragm, and two pressure cavities. The proposed CPG comprises two antagonistic diaphragm valves, such as those proposed by Rothemund, which can oscillate between a constant pressure source (P_S) and venting to the atmosphere. This is done by connecting the output of the valve to the positive bias port and relying on the hysteresis behaviour of the bi-stable diaphragm to switch between inflation and deflation states.

Consider the case for two actuators with internal pressure (P_A and P_B), and a single pressure source (P_S). Figure 8 shows the configuration of the soft CPG. At the centre of the valve is a conical bi-stable diaphragm, with a flat centre disk to facilitate pass-through of the buckling tubes. This design uses three buckling tubes, two shorter tubes that connect the pressure supply, and one longer tube allowing for venting. There are six ports, two that vent to the atmosphere (P_{atm}), two that connect to the pressure supply (P_S), and two output ports (P_A and P_B). The design further calls for two pressurised cavities separated by the diaphragm that, when charged, switch the position of the diaphragm. The design of the buckling tubes, diaphragm, and pressure cavities are dependent on each other.

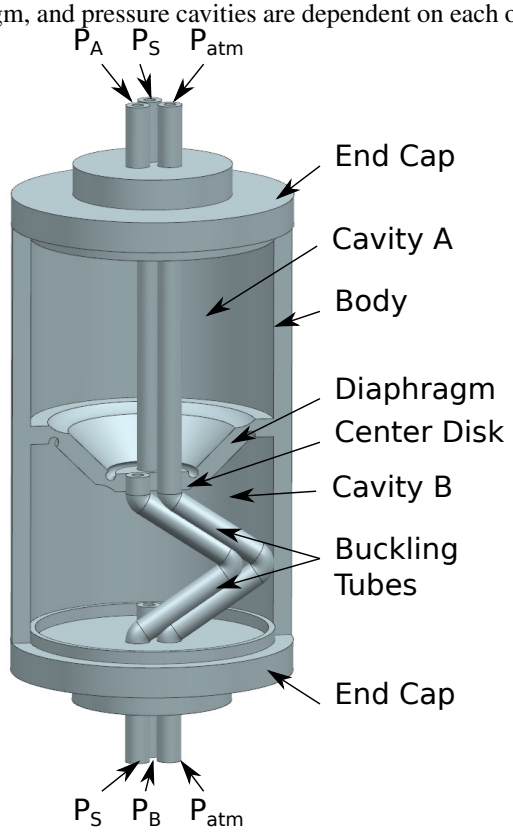

Figure 8 Soft CPG schematic and parts. The schematic shows the CPG having a single cast body forming the walls and diaphragm. Two endcaps complete cavities A and B. Five supply lines, supply pressure (P_S), atmospheric pressure (P_{atm}), pressure in cavity A (P_A), and pressure in cavity B (P_B are indicated on each input line.

3.1 Buckling Tubes

Although it is possible to use a simple relationship to predict the load required to buckle a slender tube, no simple relationship describes the point at which a tube inhibits airflow when used as a pinch valve. Therefore, a simple test is conducted under fixed-fixed end conditions to determine the buckled length of tubes at the point where the tube pinches closed and prevent airflow. Five replicate tests are conducted for tubes ranging from 20 to 40 mm long made from the two candidate materials. Fitting a line to the results for each material creates a useful design tool, with the correlation coefficients for the Mould Star 30 and Smooth-Sil 950 being 0.989 and 0.999, respectively. In a general application, the designer needs to experiment with each tube diameter and thickness. However, acknowledging the linear relationship between initial length and critical length for each tube can reduce the number of experiments needed.

The presented design needs five tubes in total, two output tubes connected to P_A and P_B, two tubes connecting the supply pressure P_S to each of the internal cavities, and one tube passing through the entire body to allow for venting to the atmosphere P_{atm}. Only the supply and venting tubes buckle to act as pinch valves controlling airflow through cavities A and B. The supply tubes each pass directly through the centre of the conical diaphragm. When unbuckled, the supply tube passing through cavity A allows flow through cavity B. When the diaphragm switches, the tube in cavity A buckles and stops supplying to cavity B. The reverse is valid for the supply tube passing through cavity B.

The venting tube passes through both cavity A and B with two holes punched through it on either side of the centre disk of the diaphragm. When buckled, the portion of the venting tube in cavity A prohibits venting from cavity A. When unbuckled, venting is allowed.

3.2 Bi-stable Diaphram

A bi-stable diaphragm secures the buckling tubes, acting as both a manifold for distributing the airflow internally and the actuator, buckling the tubes. The bi-stable nature of the diaphragm holds the valve in one of two distinct states. Unlike the Rothmund valves, the CPG makes use of a conical diaphragm, Figure 9. This configuration provides a flat centre disk for the mounting and pass-through of buckling tubes, and the addition of the dedicated 'hinge' regions means that the snap-through characteristic of the diaphragm can be maintained with less dependence on the stiffness of the material chosen. The design features for the diaphragm are the inner disk diameter, diameter, thickness, and hinge undercuts.

The centre disk needs to be larger than twice the outer diameter of the buckling tubes, with three tubes attaching directly to this flat surface. The diameter is a compromise between the stroke required to buckle the internal tubes and the conical angle. Deep cones have allowed for more stroke within a narrower body but require higher pressures to switch between positions. Shallow cones allow for less stroke at a given diameter but require a lower switching pressure. A designer can choose either the outer diameter of the diaphragm or the buck-

http://dx.doi.org/10.69694/2309-8988/2025/v41a3

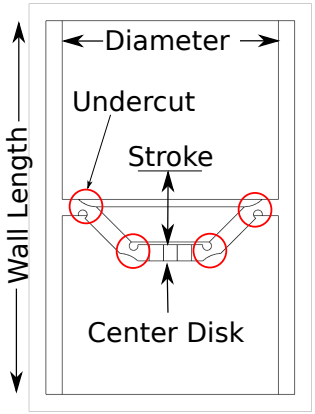

Figure 9 Detailed view of the central body of the CPG containing the bi-stable diaphragm. Undercut regions are highlighted in red circles.

ling tube length first, depending on the design priority. It is, however, important that the stroke provided by articulating the diaphragm exceeds the difference between the initial and critical length of the chosen buckling tube. The diaphragm and undercut thickness are selected together. The undercut reduces the diaphragm thickness to one-third. The hinge is responsible for the improved articulation of the diaphragm, allowing for a thicker membrane than the Rothmund valves.

3.3 Pressure Cavities

The soft CPG requires two internal cavities to connect to the pressure supply and vent to the atmosphere, depending on the position of the diaphragm. The pressure cavities have three design parameters: the wall length, diameter, and thickness, Figure 9. The sum of the critical tube length, initial tube length, and centre disk thickness determines the wall length. Wall thickness needs to be sufficient to maintain the overall shape of the CPG, and the diameter of the diaphragm defines the internal diameter of the body.

4 Results

The fabricated CPG is connected to the pneumatic test bench to evaluate whether both output ports produce oscillating pressure. Figure 10 shows a sequence of images taken during operation. Two accumulators are connected to the CPG, representing two pneumatic actuators to be controlled. Under regular operation, both accumulators inflate, and their inflation is out of phase. However, when the input pressure exceeds a critical level, both accumulators are inflated and remain static. This gives the proposed CPG three modes of operation. First, where both actuators are discharged and compliant. Second, when each actuator is charged out of sync with the other, it potentially forms a walking gait. Third, both actuators are charged and rigid, potentially a swimming gait. In addition to the alternating pressurisation we observed that when the input pressure exceeds a critical value, both actuators inflate.

A numerical optimiser using a least-squares performance measure results is used to fit a single-term Fourier series to the recorded line pressure of accumulators A and B. Each accumulator undergoes a pressure oscillation that is out of phase with the other when connected to a regulated supply. The pressure data is first detrended before determining the frequency and phase angle of the pressure oscillation. A 30-second rolling window is applied to the data and analysed with a Fast Fourier Transform (FFT). The Fourier fit and FFT show accumulator A pulses with an amplitude of 4.5 kPa and 10.0 kPa offset, while accumulator B pulses with an amplitude of 5.4 kPa and 8.5 kPa offset when subjected to a regulated supply at 20 kPa. The oscillation frequency is 0.099 Hz, and actuator B lags actuator A by 183 degrees. It is important to note that the purpose of the FFT here is not to determine the exact shape of the pressure pulse but rather the overall performance measures of frequency and amplitude.

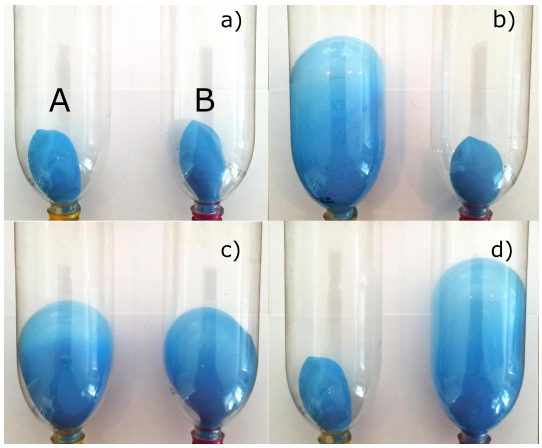

Figure 10 Soft CPG connected to the pneumatic test bench, accumulator 'A' left and accumulator 'B' right. a) Both accumulators start the test deflated. b) Accumulator 'A' inflates while accumulator 'B' remains deflated. When accumulator A reaches full inflation, the pressure in it triggers the bi-stable diaphragm to switch, c) allowing accumulator A to vent to the atmosphere while accumulator B inflates. d) Accumulator 'A' continues to deflate to atmospheric pressure while accumulator 'B' reaches full inflation, triggering the diaphragm to switch.

Increasing the input pressure from 20 kPa, 24 kPa to 28 kPa shows the dependence of oscillation frequency on input pressure. Ten replicate tests were conducted at each pressure. The increased supply pressure increases the frequency of oscillation from 0.10 Hz, to 0.14 Hz and 0.24 Hz, respectively. Figure 11 shows no overlap in the measured data for each of the three pressures. When the input pressure exceeds a critical value, the oscillating output ceases, and both actuators become statically pressurised.

5 Conclusion

This paper presents a design concept and fabrication process for a soft central pattern generator. The soft CPG converts a constant pressure input to two oscillating outputs within a single valve. The more compliant bi-stable diaphragm mechanism design reduced the dependence on material properties in determining the switching pressure. It allowed the two output lines to pulse with similar maximum and nominal pressures.

http://dx.doi.org/10.69694/2309-8988/2025/v41a3

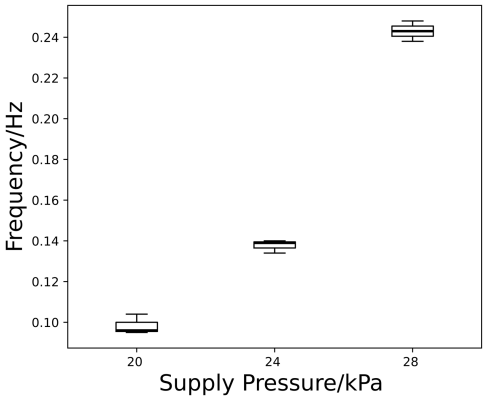

Figure 11 Accumulator oscillation frequency with increasing supply pressure. The thicker centre line indicates the mean value, the box is the inter-quartile range, and the whiskers indicate the minimum and maximum values.

As a result, the output of each line is out of phase, producing a rhythmic switching between pressurising two actuators. In addition, changes in the input pressure adjust the oscillation frequency between the two output channels.

The proposed CPG allows for effective decentralised, autonomous control of paired actuators, capable of alternately pressurising two actuators. This capability is well-suited to controlling rhythmically actuated antagonistic pairs of actuators standard in biomimetic locomotion. In the case of mimicking the three salamander gaits, the consolidation of antagonistic pairs of actuators alone will reduce the required degree of control from 16 independent actuators to 8 pairs, each connected to a single universal supply and control line. Further, changing the supply pressure controls the speed of locomotion. Changing gaits are facilitated by the static pressurisation of actuator pairs when the supply pressure exceeds the critical pressure for a CPG.

The proposed design produces a functioning soft central pattern generator that 1) autonomously produces a pair of oscillating outputs 2) that are out of phase 3) from a single constant input, 4) with adjustable frequency, and 5) a non-linear switch from dynamic motion to static inflation. In practice, this allows a designer to control the locomotion speed of a simple quadruped robot, such as the 'multigait' robot, by increasing the single control pressure and changing gait by exceeding a critical pressure.

Fabrication of this CPG is relatively simple to achieve using methods familiar to the soft robotics community. Casting into 3D printed moulds produces the individual components, which are manually assembled and glued into place; however, access to 3D elastomer printers may simplify this process.

The soft central pattern generator reduces the number of control signals needed to actuate a soft robot and allows for decentralised control without electronic control. The device is suited to the employment of cycled antagonistic actuators that experience significant bending, compressive or tensile strain. The design does not rely on rigid components. It functions well in wet environments or those with strong magnetic or radiative fields, and the decentralised control contributes meaningfully to the robustness of soft robots.

This research was funded by the National Research Foundation of South Africa grant number 129381.

References

[1] K. C. Galloway, K. P. Becker, B. Phillips, J. Kirby, S. Licht, D. Tchernov, R. J. Wood, and D. F. Gruber, "Soft Robotic Grippers for Biological Sampling on Deep Reefs," *Soft Robotics*, vol. 3, no. 1, pp. 23–33, 2016.

[2] N. Cheng, J. Amend, T. Farrell, D. Latour, C. Martinez, J. Johansson, A. McNicoll, M. Wartenberg, S. Naseef, W. Hanson, and W. Culley, "Prosthetic Jamming Terminal Device: A Case Study of Untethered Soft Robotics," *Soft Robotics*, vol. 3, no. 4, pp. 213–222, 2016.

[3] P. Polygerinos, S. Lyne, Z. Wang, L. F. Nicolini, B. Mosadegh, G. M. Whitesides, and C. J. Walsh, "Towards a soft pneumatic glove for hand rehabilitation," in *IEEE International Conference on Intelligent Robots and Systems*, (Tokyo, Japan), pp. 1512–1517, IEEE, 2013.

[4] M. Calisti, M. Giorelli, G. Levy, B. Mazzolai, B. Hochner, C. Laschi, and P. Dario, "An octopus-bioinspired solution to movement and manipulation for soft robots," *Bioinspiration and Biomimetics*, vol. 6, no. 3, p. 036002, 2011.

[5] A. Menciassi, S. Gorini, G. Pernorio, and P. Dario, "A SMA actuated artificial earthworm," *Proceedings - IEEE International Conference on Robotics and Automation*, vol. 2004, no. 4, pp. 3282–3287, 2004.

[6] H. T. Lin, G. G. Leisk, and B. Trimmer, "GoQBot: A caterpillar-inspired soft-bodied rolling robot," *Bioinspiration and Biomimetics*, vol. 6, no. 2, p. 026007, 2011.

[7] D. Trivedi, C. D. Rahn, W. M. Kier, and I. D. Walker, "Soft robotics: Biological inspiration, state of the art, and future research," *Applied Bionics and Biomechanics*, vol. 5, no. 3, pp. 99–117, 2008.

[8] C. Laschi and M. Cianchetti, "oft robotics: New perspectives for robot bodyware and control," *Frontiers in Bioengineering and Biotechnology*, vol. 2, no. JAN, pp. 1–5, 2014.

[9] P. Polygerinos, N. Correll, S. A. Morin, B. Mosadegh, C. D. Onal, K. Petersen, M. Cianchetti, M. T. Tolley, and R. F. Shepherd, "Soft Robotics: Review of Fluid-Driven Intrinsically Soft Devices; Manufacturing, Sensing, Control, and Applications in Human-Robot Interaction," *Advanced Engineering Materials*, vol. 19, no. 12, p. 1700016, 2017.

http://dx.doi.org/10.69694/2309-8988/2025/v41a3

[10] C. Laschi, B. Mazzolai, and M. Cianchetti, "Soft robotics: Technologies and systems pushing the boundaries of robot abilities," *Science Robotics*, vol. 1, no. 1, p. eaah3690, 2016.

[11] D. Rus and M. T. Tolley, "Design, fabrication and control of soft robots," *Nature*, vol. 521, no. 7553, pp. 467–475, 2015.

[12] F. Connolly, C. J. Walsh, and K. Bertoldi, "Automatic design of fiber-reinforced soft actuators for trajectory matching," *Proceedings of the National Academy of Sciences of the United States of America*, vol. 114, no. 1, pp. 51–56, 2017.

[13] H. Zhao, K. O'Brien, S. Li, and R. F. Shepherd, "Optoelectronically innervated soft prosthetic hand via stretchable optical waveguides," *Science Robotics*, vol. 1, no. 1, pp. 1–10, 2016.

[14] Y. L. Park, B. R. Chen, and R. J. Wood, "Design and fabrication of soft artificial skin using embedded microchannels and liquid conductors," *IEEE Sensors Journal*, vol. 12, no. 8, pp. 2711–2718, 2012.

[15] R. Adam Bilodeau, E. L. White, and R. K. Kramer, "Monolithic fabrication of sensors and actuators in a soft robotic gripper," *IEEE International Conference on Intelligent Robots and Systems*, vol. 2015-December, pp. 2324–2329, 2015.

[16] J. Y. Sun, C. Keplinger, G. M. Whitesides, and Z. Suo, "Ionic skin," *Advanced Materials*, vol. 26, no. 45, pp. 7608–7614, 2014.

[17] S. Gillner, and P. Wallen, "Central pattern generators for locomotion, with special reference to vertebrates," *Annual review of neuroscience*, vol. 8, no. 1, pp. 233–261, 1985.

[18] A. Bicanski, D. Ryczko, J. M. Cabelguen, and A. J. Ijspeert, "From lamprey to salamander: An exploratory modeling study on the architecture of the spinal locomotor networks in the salamander," *Biological Cybernetics*, vol. 107, no. 5, pp. 565–587, 2013.

[19] N. Harischandra, J. M. Cabelguen, and Ö. Ekeberg, "A 3D musculo-mechanical model of the salamander for the study of different gaits and modes of locomotion," *Frontiers in Neurorobotics*, vol. 4, no. DEC, pp. 1–10, 2010.

[20] J. T. Buchanan and D. R. McPherson, "The neuronal network for locomotion in the lamprey spinal cord: Evidence for the involvement of commissural interneurons," *Journal of Physiology - Paris*, vol. 89, no. 4-6, pp. 221–233, 1995.

[21] A. Bicanski, D. Ryczko, J. Knuesel, N. Harischandra, V. Charrier, Ö. Ekeberg, J. M. Cabelguen, and A. J. Ijspeert, "Decoding the mechanisms of gait generation in salamanders by combining neurobiology, modeling and robotics," *Biological Cybernetics*, vol. 107, no. 5, pp. 545–564, 2013.

[22] A. Kyriakatos, R. Mahmood, J. Ausborn, C. P. Porres, A. Büschges, and A. E. Manira, "Initiation of locomotion in adult Zebrafish," *Journal of Neuroscience*, vol. 31, no. 23, pp. 8422–8431, 2011.

[23] D. Ryczko, F. Auclair, J. M. Cabelguen, and R. Dubuc, "The mesencephalic locomotor region sends a bilateral glutamatergic drive to hindbrain reticulospinal neurons in a tetrapod," *Journal of Comparative Neurology*, vol. 524, no. 7, pp. 1361–1383, 2016.

[24] A. J. Ijspeert, A. Crespi, D. Ryczko, and J. M. Cabelguen, "From swimming to walking with a salamander robot driven by a spinal cord model," *Science*, vol. 315, no. 5817, pp. 1416–1420, 2007.

[25] A. A. Faudzi, M. R. Razif, G. Endo, H. Nabae, and K. Suzumori, "Soft-Amphibious robot using thin and soft McKibben actuator," *IEEE/ASME International Conference on Advanced Intelligent Mechatronics, AIM*, pp. 981–986, 2017.

[26] C. Paul, "Morphological computation. A basis for the analysis of morphology and control requirements," *Robotics and Autonomous Systems*, vol. 54, no. 8, pp. 619–630, 2006.

[27] B. Mosadegh, P. Polygerinos, C. Keplinger, S. Wennstedt, R. F. Shepherd, U. Gupta, J. Shim, K. Bertoldi, C. J. Walsh, and G. M. Whitesides, "Pneumatic networks for soft robotics that actuate rapidly," *Advanced Functional Materials*, vol. 24, no. 15, pp. 2163–2170, 2014.

[28] R. V. Martinez, J. L. Branch, C. R. Fish, L. Jin, R. F. Shepherd, R. M. D. Nunes, Z. Suo, and G. M. Whitesides, "Robotic tentacles with three-dimensional mobility based on flexible elastomers," *Advanced Materials*, vol. 25, no. 2, pp. 205–212, 2013.

[29] D. Yang, M. S. Verma, J.-H. So, B. Mosadegh, C. Keplinger, B. Lee, F. Khashai, E. Lossner, Z. Suo, and G. M. Whitesides, "Buckling Pneumatic Linear Actuators Inspired by Muscle," *Advanced Materials Technologies*, vol. 1, no. 3, p. 1600055, 2016.

[30] F. Iida and C. Laschi, "Soft robotics: Challenges and perspectives," *Procedia Computer Science*, vol. 7, pp. 99–102, 2011.

[31] F. Ilievski, A. D. Mazzeo, R. F. Shepherd, X. Chen, and G. M. Whitesides, "Soft robotics for chemists," *Angewandte Chemie - International Edition*, vol. 123, pp. 1930–1935, 2011.

[32] R. F. Shepherd, F. Ilievski, W. Choi, S. a. Morin, A. A. Stokes, A. D. Mazzeo, X. Chen, M. Wang, and G. M. Whitesides, "Multigait soft robot," *Proceedings of the National Academy of Sciences*, vol. 108, no. 51, pp. 20400–20403, 2011.

http://dx.doi.org/10.69694/2309-8988/2025/v41a3

[33] P. Paoletti, G. W. Jones, and L. Mahadevan, "Grasping with a soft glove: Intrinsic impedance control in pneumatic actuators," *Journal of the Royal Society Interface*, vol. 14, no. 128, 2017.

[34] M. T. Tolley, R. F. Shepherd, B. Mosadegh, K. C. Galloway, M. Wehner, M. Karpelson, R. J. Wood, and G. M. Whitesides, "A Resilient, Untethered Soft Robot," *Soft Robotics*, vol. 1, no. 3, pp. 213–223, 2014.

[35] A. D. Marchese, C. D. Onal, and D. Rus, "Soft robot actuators using energy-efficient valves controlled by electropermanent magnets," *IEEE International Conference on Intelligent Robots and Systems*, no. 1, pp. 756–761, 2011.

[36] B. Mosadegh, A. D. Mazzeo, R. F. Shepherd, S. a. Morin, U. Gupta, I. Z. Sani, D. Lai, S. Takayama, and G. M. Whitesides, "Control of soft machines using actuators operated by a Braille display.," *Lab on a chip*, vol. 14, no. 1, pp. 189–99, 2014.

[37] M. Wehner, R. L. Truby, D. J. Fitzgerald, B. Mosadegh, G. M. Whitesides, J. A. Lewis, and R. J. Wood, "An integrated design and fabrication strategy for entirely soft, autonomous robots," *Nature*, vol. 536, no. 7617, pp. 451–455, 2016.

[38] B. Mosadegh, C. H. Kuo, Y. C. Tung, Y. S. Torisawa, T. Bersano-Begey, H. Tavana, and S. Takayama, "Integrated elastomeric components for autonomous regulation of sequential and oscillatory flow switching in microfluidic devices," *Nature Physics*, vol. 6, no. 6, pp. 433–437, 2010.

[39] H. Badr, C. L. Carmack, D. A. Kashy, M. Cristofanilli, and T. A. Revenson, "Microfluidic Pneumatic Logic Circuits and Digital Pneumatic Microprocessors," *Lab on a chip*, vol. 9, no. 21, pp. 3131–3143, 2009.

[40] Q. Zhang, M. Zhang, L. Djeghlaf, J. Bataille, J. Gamby, A. M. Haghiri-Gosnet, and A. Pallandre, "Logic digital fluidic in miniaturized functional devices: Perspective to the next generation of microfluidic lab-on-chips," *Electrophoresis*, vol. 38, no. 7, pp. 953–976, 2017.

[41] M. A. Unger, H. P. Chou, T. Thorsen, A. Scherer, and S. R. Quake, "Monolithic microfabricated valves and pumps by multilayer soft lithography," *Science*, vol. 288, no. 5463, pp. 113–116, 2000.

[42] N. Napp, B. Araki, M. T. Tolley, R. Nagpal, and R. J. Wood, "Simple passive valves for addressable pneumatic actuation," in *Proceedings - IEEE International Conference on Robotics and Automation*, pp. 1440–1445, 2014.

[43] R. F. Shepherd, A. A. Stokes, J. Freake, J. Barber, P. W. Snyder, A. D. Mazzeo, L. Cademartiri, S. A. Morin, and G. M. Whitesides, "Using explosions to power a soft robot," *Angewandte Chemie - International Edition*, vol. 52, no. 10, pp. 2892–2896, 2013.

[44] S. T. Mahon, A. Buchoux, M. E. Sayed, L. Teng, and A. A. Stokes, "Soft robots for extreme environments: Removing electronic control," *RoboSoft 2019 - 2019 IEEE International Conference on Soft Robotics*, pp. 782–787, 2019

[45] P. Rothemund, A. Ainla, L. Belding, D. J. Preston, S. Kurihara, Z. Suo, and G. M. Whitesides, "A soft, bistable valve for autonomous control of soft actuators," *Science Robotics*, vol. 3, no. 16, p. eaar7986, 2018.

[46] D. J. Preston, H. J. Jiang, V. Sanchez, P. Rothemund, J. Rawson, M. P. Nemitz, W. K. Lee, Z. Suo, C. J. Walsh, and G. M. Whitesides, "A soft ring oscillator," *Science Robotics*, vol. 4, no. 31, pp. 1–10, 2019.

[47] D. Drotman, S. Jadhav, D. Sharp, C. Chan, and M. T. Tolley, "Electronics-free pneumatic circuits for controlling soft-legged robots," *Science Robotics*, vol. 6, no. 51, pp. 1–12, 2021.

[48] D. J. Preston, P. Rothemund, H. J. Jiang, M. P. Nemitz, J. Rawson, Z. Suo, and G. M. Whitesides, "Digital logic for soft devices," *Proceedings of the National Academy of Sciences of the United States of America*, , vol. 116, no. 16, pp. 7750–7759, 2019.

[49] K. Xu, and N. O. Perez-Arancibia, "Electronics-Free Logic Circuits for Localized Feedback Control of Multi-Actuator Soft Robots," *IEEE Robotics and Automation Letters*, , vol. 5, no. 3, pp. 3990–3997, 2020.

http://dx.doi.org/10.69694/2309-8988/2025/v41a3